Towards testing sterile neutrino dark matter with the *Spectrum-Roentgen-Gamma* mission

V. V. Barinov,[1,2,*] R. A. Burenin,[3,4,†] D. S. Gorbunov,[2,5,‡] and R. A. Krivonos[3,§]

[1]*Physics Department, M. V. Lomonosov Moscow State University, Leninskie Gory, Moscow 119991, Russia*
[2]*Institute for Nuclear Research of the Russian Academy of Sciences, Moscow 117312, Russia*
[3]*Space Research Institute of the Russian Academy of Sciences, Moscow 117997, Russia*
[4]*National Research University Higher School of Economics, Moscow 101000, Russia*
[5]*Moscow Institute of Physics and Technology, Dolgoprudny 141700, Russia*

(Received 20 July 2020; accepted 18 February 2021; published 15 March 2021)

We investigate the prospects of the *Spectrum-Roentgen-Gamma* (*SRG*) mission in search for the keV-scale mass sterile neutrino dark matter radiatively decaying into active neutrinos and photons. The ongoing all-sky x-ray survey of the *SRG* space observatory with data acquired by the *ART-XC* and *eROSITA* telescopes can provide a possibility to fully explore the resonant production mechanism of the dark matter sterile neutrino, which exploits the lepton asymmetry in the primordial plasma consistent with cosmological limits from the big bang nucleosynthesis. In particular, it is shown that at the end of the four year all-sky survey, the sensitivity of the *eROSITA* telescope near the 3.5 keV line signal reported earlier can be comparable to that of the *XMM*-Newton with all collected data, which will allow one to carry out another independent study of the possible sterile neutrino decay signal in this area. In the energy range below ≈2.4 keV, the expected constraints on the model parameters can be significantly stronger than those obtained with the *XMM*-Newton. From the *ART-XC* data, in the energy range approximately from 5 to 20 keV, it can be possible to get more stringent constraints than those obtained with *NuSTAR* so far. We conclude that the *SRG* mission has a very high potential in testing the sterile neutrino dark matter hypothesis.

DOI: 10.1103/PhysRevD.103.063512

I. INTRODUCTION

The recently launched *Spectrum-Roentgen-Gamma* space observatory (Spektr-RG or *SRG*, [1]), carrying two x-ray telescopes on board, *Mikhail Pavlinsky ART-XC* [2–6] and *eROSITA* [7–9], is expected to contribute considerably to cosmology by investigating cosmic large scale structure properties associated with galaxy clusters [7,8,10,11], providing a major improvement in cosmological constraints as compared to the results from earlier x-ray, Sunyaev-Zeldovich, and optical galaxy cluster surveys, e.g., [12–14]. While these studies can further refine the parameters of the standard cosmological model (presently, ΛCDM), the *SRG* has also high potential in testing specific particle physics models of dark energy and dark matter. Notably, dark matter particles decaying or annihilating with keV-scale photons in the final state can be probed with *eROSITA* (energy range 0.2–10 keV) and *ART-XC* (4–30 keV) x-ray telescopes aboard *SRG*.

In this paper we concentrate on a particular candidate of dark matter—sterile neutrinos—unstable because of mixing with active neutrinos and consequently exhibiting a two-body radiative decay into active neutrino (electron, muon, or tau neutrino) and photon

$$\nu_s \to \nu_{e,\mu,\tau} + \gamma, \tag{1}$$

with the decay rate [15,16]

$$\Gamma_\gamma = \frac{9}{1024}\frac{\alpha}{\pi^4} G_F^2 m_s^5 \sin^2 2\theta, \\ = 1.36 \times 10^{-22} \left(\frac{m_s}{1\ \text{keV}}\right)^5 \sin^2 2\theta\ \text{s}^{-1}, \tag{2}$$

where m_s is the sterile neutrino mass, and θ is the sterile-active mixing angle; for small mixing there is no need to distinguish between the mass and flavor states of the sterile fermion. The outgoing photon energy is $E_\gamma = m_s/2$, and for sterile neutrinos forming galactic dark matter the expected photon spectrum is highly monochromatic with width of order the velocity of the dark matter particles in the galaxy, i.e., $v \sim 10^{-4}$–10^{-3}. This suggests a signature in the

*barinov.vvl@gmail.com
†rodion@hea.iki.rssi.ru
‡gorby@ms2.inr.ac.ru
§krivonos@cosmos.ru

galactic photon spectrum [17] to be searched for by the x-ray telescopes.

In the simplest models the sterile neutrinos are Majorana fermions, singlets with respect to the gauge group of the Standard Model (SM) of particle physics. The introduction of sterile neutrinos into particle physics is motivated primarily by their contribution to the active neutrino masses coming (after electroweak symmetry breaking) from Yukawa-type interactions with the SM Higgs doublet and lepton doublets. To provide all the three active neutrinos with masses, one needs at least three sterile neutrinos, but the lightest (or fourth, fifth, etc.) can be sufficiently feebly coupled and hence long-lived to form dark matter, see Refs. [18,19] for a review. Naturally, this strong physical motivation makes the model very attractive phenomenologically [20] and the suggested signature has been exploited by x-ray telescopes to explore the relevant part of model parameter space (m_s, θ). The absence of monochromatic photons of a given frequency implies an upper limit on the mixing angle at the sterile neutrino mass equal to the double photon frequency provided by Eq. (2). The latest results are provided by the *NuSTAR* experiment, see Fig. 1 for relevant astrophysical and cosmological constraints.

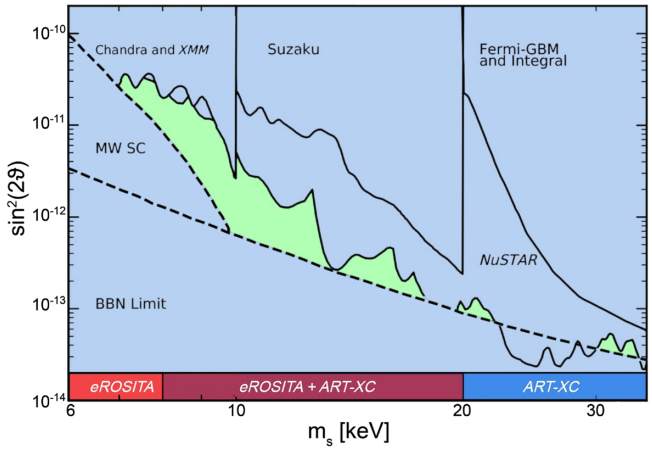

FIG. 1. Constraints on the parameters of sterile neutrinos: the summary plot is adopted from Ref. [21]. The green color indicates the allowed region of sterile neutrino parameter space consistent with x-ray searches (solid lines indicate the upper limits), cosmological limits from big bang nucleosynthesis (BBN) (dashed line refers to the lower bounds) and cosmological constraints from MW satellite galaxy counts (dashed line). The x-ray bounds are weaker if the sterile neutrinos form only a subdominant component of dark matter. The limits from galaxy counts largely depend also on the sterile neutrino spectrum, and hence on its production mechanism operating in the early Universe. The BBN limits may be relaxed in an extended model, e.g. with more ingredients in the neutrino sector. The red color shows the energy range $(E_\gamma = m_s/2)$ covered by the *eROSITA* telescope; the blue shows the energy range covered by the *ART-XC* telescope; the purple refers to the overlapping region of the energy ranges of these two telescopes.

As a component being in thermal equilibrium with primordial plasma in the early Universe, the sterile neutrino that makes all dark matter is not suitable because it has the same (qualitative) problems with cosmic structure formation as active neutrinos have. However, sterile neutrinos can be produced nonthermally by active neutrinos oscillating in the primordial plasma, which works with relatively small mixing. Note that the simplest case, where the mixing is in one-to-one correspondence with the relic sterile neutrino abundance [22], has been already excluded [19]. Nevertheless, for the efficient production of sterile neutrinos in the early Universe, a much smaller mixing [below upper x-ray limits on (2)] is still sufficient in cosmological models with lepton asymmetry in the primordial plasma [23] or physical model extensions, see, e.g., Refs. [24–26] for scalars coupled to sterile neutrinos. Along with particle physics motivations, these model extensions are supported by a feature at near 3.5 keV, which claimed to be observed in spectra of several dark matter dominated astrophysical objects [27,28] (see, however, [29–31]). Therefore, hunts for a monochromatic line in cosmic x-rays, presumably initiated by decays (1), remain worthwhile and promising in regards to revealing the nature of dark matter. In this paper we estimate the sensitivity of *SRG* telescopes to the models with sterile neutrino dark matter.

If dark matter consists of the decaying sterile neutrinos, then we expect to observe correlated signal fluxes from various dark matter dominated astronomical objects. In this paper, we consider the Galactic Center (GC), the Andromeda galaxy (M31), and the Draco dwarf galaxy as possible sources of the monochromatic photons. This choice is motivated by investigations based on analyses of previous generation x-ray telescopes, which found them as the most prospective sources of the monochromatic line and scrutinized their dark matter structure.

II. EXPECTED SIGNAL

Assuming that the sterile neutrinos form (a part of) galactic dark matter, we can estimate the photon flux from decays (1) in a nearby source (e.g., Galactic Center, a Milky Way satellite, a local group member) as follows,

$$F_{\rm DM} = \frac{1}{4\pi}\frac{\Gamma_\gamma}{m_s}\mathcal{S}_{\rm DM}. \tag{3}$$

Here $\mathcal{S}_{\rm DM}$ is the sterile neutrino dark matter (DM) column density of the observed object along the line of sight in the given circular field of view (FOV) towards the center of dark halo of the object,

$$\mathcal{S}_{\rm DM} = \int_0^{2\pi}\int_0^{w_r}\int_{l_{\rm min}}^{l_{\rm max}} \frac{\rho_{\rm DM}(r(l,\psi))}{l^2} l^2 \sin\psi {\rm d}\phi {\rm d}\psi {\rm d}l, \tag{4}$$

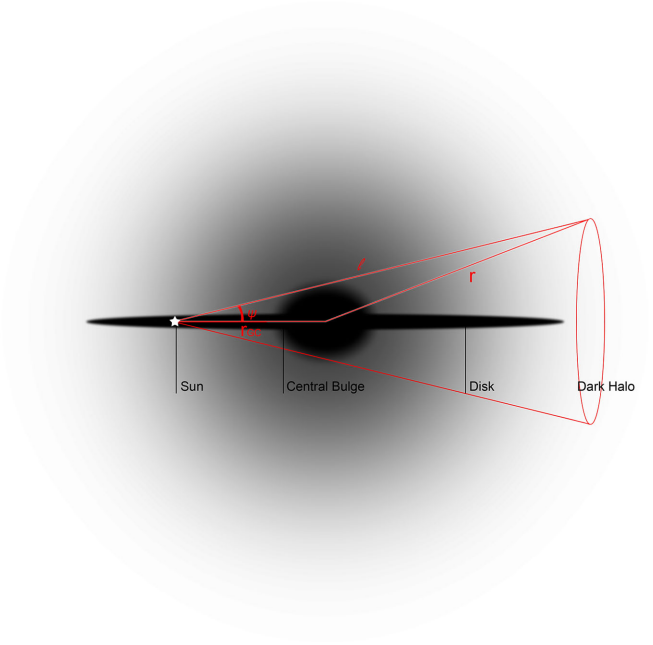

FIG. 2. Sketch illustrating the signal geometry when the Galaxy halo is observed.

where w_r is the FOV radius of telescope, $\rho_{\rm DM}(r(l,\psi))$ is the dark matter density profile, and $r(l,\psi) = \sqrt{R^2 - 2Rl\cos\psi + l^2}$, ψ is the angle between the line of sight and direction to the center of the object, R is the distance from the observer to the center of the dark matter halo, e.g., distance to the Galaxy center in the case of Milky Way, l is the distance along the line of sight,[1] see Fig. 2. Thus, the photon flux from the sterile neutrino decays (1) is given by the following expression:

$$F_{\rm DM} = \frac{1}{7.88\times10^{-4}}\left(\frac{S_{\rm DM}}{\rm M_\odot pc^{-2}}\right)\left(\frac{2E_\gamma}{1\ \rm keV}\right)^4 \sin^2 2\theta \frac{\rm cts}{\rm cm^2\ s}. \tag{5}$$

To evaluate the signal flux, we need to know the distribution density of dark matter for each object, which is the source of the photons, under study. This quantity is neither fixed from the theory, nor directly measured, and so it has many uncertainties. However, they are not so dramatic for the decay signal, as compared to the annihilation of the dark matter particles, which signal is proportional to squared dark matter density. In our study, for MW and for M31, we use the standard NFW profile: $\rho(r) = \rho_s/(r/r_s)(1+r/r_s)^2$ [32]. For MW, we use the parameters given in Ref. [33], where the values of the scale density and scale radius are $\rho_s = 10.5\times10^{-3}$ $\rm M_\odot pc^{-3}$ and $r_s = 20$ kpc, respectively, $R_{\rm GC} = 8$ kpc and $R_{\rm vir} = 200$ kpc [34]. In Fig. 3 we illustrate uncertainties in the geometrical factor $\mathcal{S}_{\rm DM}$ entering formula for the expected signal flux (3), which are associated with variance of the DM profile. At the very center of MW (small angles) the differences in the suggested MW profiles are rather dramatic. However, below, we are interested in angles exceeding one degree, where the presented uncertainties are at the level of factor of 2, which we keep in mind. For the M31 halo, we use the parameter values from [35], where $\rho_s = 11.0\times10^{-3}$ $\rm M_\odot pc^{-3}$ and $r_s = 16.5$ kpc, $R_{\rm GC} = 780$ kpc, and $R_{\rm vir} = 207$ kpc. The matter density distribution in the Draco galaxy is well described by $\rho(r) = \rho_s/(r/r_s)^\gamma(1+(r/r_s)^\alpha)^{(\beta-\gamma)/\alpha}$, with parameters $\rho_s = 18.2\times10^{-3}$ $\rm M_\odot\ pc^{-3}$, $r_s = 3.72$ kpc, and $(\alpha,\beta,\gamma) = (2.01, 6.34, 0.71)$ and $R_{\rm GC} = 76$ kpc, $R_{\rm vir} = 1.87$ kpc [36]. Similar to the MW case, the different estimates of the M31 and Draco DM profiles, see, e.g., Refs. [37–39], imply a factor of two uncertainties in the predictions for the signal flux.

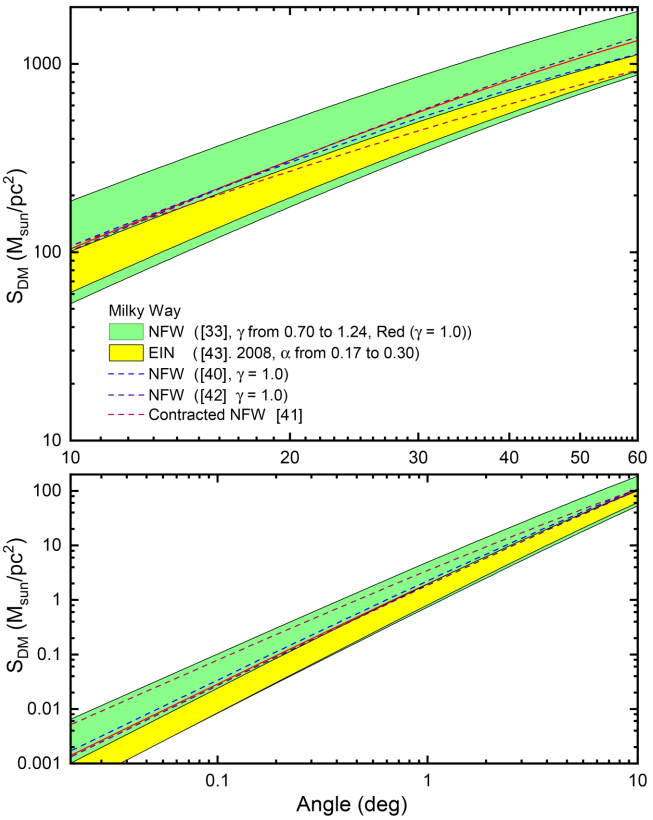

FIG. 3. Variance in the DM signal flux at a given cut on the viewing angle θ (towards the MW center) due to difference in the DM profile estimates obtained in Refs. [33,40–43].

Using the latest constraints on the parameters of sterile neutrinos presented in [21,44], we estimate the possible signal flux from these objects, and also evaluate the necessary time of observation of these objects by *SRG*

[1]For Milky Way (MW) we set $l_{\rm min} = 0$ and $l_{\rm max} \approx R + R_{\rm vir}$ and for other far objects we set $l_{\rm min} \approx R - R_{\rm vir}$ and $l_{\rm max} \approx R + R_{\rm vir}$. Multiplying the virial radius of the object $R_{\rm vir}$ by factor of two in these formulas changes the expected flux by less than 1% for M31 and about 10% for the Draco dwarf galaxy.

to strengthen the existing constraints, and to check the dark matter explanation of the 3.5 keV line.

III. *SRG* X-RAY TELESCOPES

The *Spectrum-Roentgen-Gamma* [1] is a Russian x-ray observatory created with the participation of Germany, launched in July 2019 and designed to produce a deep x-ray map of the Universe in a wide, 0.2–30 keV, energy range. Its scientific payload consists of two x-ray telescopes—*ART-XC* [2–6] and *eROSITA* [7–9]—built in Russia and Germany, respectively. A map of the large scale structure of the Universe including more than a hundred thousand clusters of galaxies will be outlined. At the end of the main survey mission (four years of operation), the *SRG* will be switched to the pointed observations of selected objects (two years), which will allow one to explore the most interesting x-ray sources in more detail. In particular, using these data, it will be possible to use the spectra of various astrophysical objects to search for the peak signature of dark matter radiative decays.

The *SRG* observatory revolves with a six-month period around the second Lagrange point (L2) of the Sun-Earth system, located at the distance of approximately 1.5 million km from Earth, in an elliptical nonclosed orbit with 0.75 million km and 0.25 million km semiaxes. In the survey mode the telescope pointing axis is continuously rotated approximately around the direction to Earth and Sun, therefore, due to this observing strategy the entire celestial sphere is covered in a six-month period, and eight full scans of the celestial sphere will be performed during the main four-year stage of operation. The full field of view of the *eROSITA* telescope is 0.8 deg^2 and for *ART-XC* is around 2 deg^2 (in telescope + concentrator mode, see [5]). This means that the total average exposure time for any part of the sky will be about 2500 s and 6100 s (uncorrected for vignetting). Note that by the end of the survey mission, the largest exposure is expected in the region of the ecliptic poles, since for each revolution the telescope axis passes near these poles.

In the survey mode, the most important parameter characterizing the ability to cover a large part of the sky is "grasp," which is defined as the product of the effective area of the telescope and the angular area of its field of view corrected for vignetting. Grasps for *eROSITA* and *ART-XC* telescopes on board *SRG* observatory, available for investigations of the sterile neutrino dark matter radiative decay signatures, are shown in Fig. 4 in comparison with those of *XMM*-Newton [45] and *NuSTAR* [46] telescopes. The grasp of the *ART-XC* telescope is shown for telescope + concentrator mode. The grasp for *XMM*-Newton is calculated using PN, MOS1, and MOS2 effective areas and vignetting taken from the *XMM*-Newton Users Handbook. The grasp for the *NuSTAR* telescope is calculated for stray-light aperture mode, used in the sterile neutrino DM decay searches [21,33]. The lower and upper curves represent

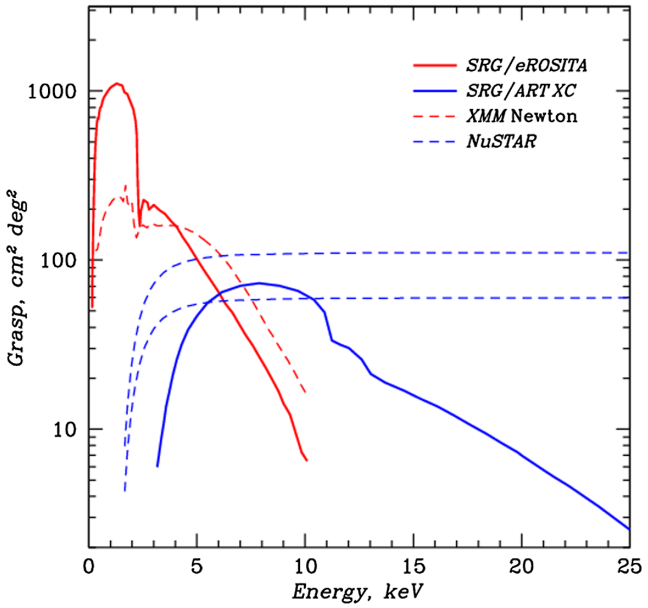

FIG. 4. Grasps for *SRG/eROSITA*, *SRG/ART-XC*, *XMM*-Newton, and *NuSTAR* telescopes, available for sterile neutrino DM decay searches. For *SRG/ART-XC* telescope grasp for telescope + concentrator mode is shown. Lower and upper *NuSTAR* grasp curves are calculated for stray-light aperture only, as used in DM search studies in the GC [33] and bulge [21], respectively (see text for details).

average *NuSTAR* side aperture (or stray-light) grasp inferred from the *NuSTAR* observations in the GC [33] and bulge [21], where the most recent DM decay constraints were achieved. The average *NuSTAR* grasp is multiplied by the energy-dependent efficiency for photons to pass through the *NuSTAR* detector beryllium shield. The difference in the *NuSTAR* grasp estimations is mainly explained by a strong stray-light contamination of bright sources in the GC. In the galactic bulge observations, *NuSTAR* stray-light aperture contamination from the x-ray background is minimized; however, the expected DM signal is also lower compared to that from the GC due to the smaller amount of DM integrated over the line of sight. Note that the total effective exposure used for the *NuSTAR* DM studies in the GC [33] and bulge [21] is ∼200 and ∼100 ks, respectively. At larger angular distances from GC the search for sterile neutrino DM decay signal was performed with higher *NuSTAR* exposure (7.5 Msec) and comparable upper limits were obtained [47].

From Fig. 4 we see that the grasp of the *eROSITA* telescope significantly supersedes that of *XMM*-Newton at the energies below ≈2.2 keV. At higher energies the grasps of the telescopes aboard *SRG* are comparable to those of *XMM*-Newton and *NuSTAR*. Therefore, the main difference in DM decay flux constraints at these energies between *eROSITA* and *ART-XC* telescopes, as compared to *XMM*-Newton and *NuSTAR*, will arise due to the difference in exposures used to observe the source. As we show below,

when the dark matter halo of our Galaxy is observed, with the *SRG* telescopes, it will be possible to collect the data with significantly higher exposures, as compared to what were used to constrain the sterile neutrino DM from *XMM-Newton* and *NuSTAR* data.

For the reliable signal detection, it is necessary to know energy dependence of the background flux. Estimates of the expected number of events for the *eROSITA* and *ART-XC* telescopes obtained by modeling the background signal and ground calibrations, as well as based on observational data from earlier missions are presented in [5,8]. The charged particles induced background, observed during the first months of the *SRG* flight, is found to be in general agreement with preflight estimates for *ART-XC* telescope [1,6] and a few times higher for *eROSITA* [1,9]. The particle background should become lower when Sun activity will be higher (e.g., [48]), which should happen during the next few years.

For the estimates below we adopt the observed particle background of *eROSITA* and *ART-XC* taken from Refs. [1,6,9]. Since the *SRG* is placed to orbit around the second Lagrange point (L2) of the Earth-Sun system, the thermal conditions onboard *SRG* and particle background on the detectors of both *ART-XC* and *eROSITA* telescopes appear to be extremely stable, as compared to those of missions at the Earth orbits.

At the energies below 2 keV, the background of the *eROSITA* telescope is dominated by cosmic x-ray background all over the sky and, additionally, by the galactic ridge x-ray emission (GRXE) [49–52] when pointed towards the Galactic plane and bulge. We expect that approximately 50% of cosmic x-ray background will be resolved by *eROSITA* at its survey limiting flux of $\sim 10^{-14}$ erg s^{-1} cm^{-2}, 0.5–2 keV, see, e.g., [53,54]. The detected x-ray sources will be removed from the data. Due to the good angular resolution of *eROSITA* and *ART-XC*, the loss of effective FOV in the extragalactic fields will not be significant, much less than 1%, which can be easily estimated given the angular resolution of the telescopes and the number of expected source detections. The loss of effective FOV due to the exclusion of bright x-ray sources near the Galactic Center will be larger, up to a few percents, which will still not be significant for our purposes. For weaker sources with flux below ∼mCrab, we calculated the contribution from the GRXE to the background model based on the near-infrared stellar mass model from Ref. [55] and 3–20 keV Galactic ridge x-ray emissivity per unit stellar mass from Ref. [49]. This approach has been proven to effectively model the observed number-flux distribution of detected sources in the Chandra deep survey of the Norma spiral arm region [56]. Note that, when analyzing the actual SRG data, the higher number of detected Galactic x-ray sources will lead, on the one side, to larger FOV losses, and, on the other side, to decreased GRXE contribution to the background model.

TABLE I. Telescopes technical performance.

	eROSITA	*ART-XC*
Energy range [keV]	0.2–10	4–30
Energy resolution, FWHM	138 eV at 6 keV	10% at 14 keV
FOV [deg^2]	0.833	0.3–2.0[a]

[a]FOV [deg^2]: Telescope 0.31, Concentrator 1.7, Full 2.0 [3–5].

The systematic uncertainties due to the background modeling are neglected here. We note however that to obtain the constraints discussed below the systematic uncertainties should be controlled at the level of ∼1%. We expect that these uncertainties in SRG telescopes data will be lower as compared to those in previous experiments, because the observed particle background is found to be very stable and it will be possible to obtain direct and accurate background measurements for both telescopes. Further details of SRG telescopes background modeling will be discussed in our future papers.

We also assume that the sterile neutrino DM decay flux is detected in a bandwidth equal to the energy resolution of the corresponding telescope, which are taken from [8] for *SRG/eROSITA* and from [3] for *SRG/ART-XC* and are summarized in Table I.

IV. RESULTS: EXPECTED CONSTRAINTS ON THE DARK MATTER DECAY FLUX

The existing constraints on the parameters of sterile neutrinos, presented in Ref. [21], can be used to estimate the ranges of possible signal flux from decays of resonantly produced dark matter sterile neutrino to be observed by the *SRG* mission. For this purpose, we calculate the photon flux (5) from decays of sterile neutrinos in the central part of MW, M31, and Draco. The corresponding sterile neutrino dark matter column density factors for MW, M31, and Draco for particular circular region radii in the formula for signal flux (5) are obtained in this way as (in $M_\odot \mathrm{pc}^{-2}$)

$$S_{\mathrm{DM}}^{\mathrm{GC}_{3.0^\circ}} = 13.7, \qquad S_{\mathrm{DM}}^{\mathrm{GC}_{60^\circ}} = 1.3 \times 10^3,$$
$$S_{\mathrm{DM}}^{\mathrm{M31}_{1.5^\circ}} = 0.39, \qquad S_{\mathrm{DM}}^{\mathrm{Draco}_{0.25^\circ}} = 1.4 \times 10^{-2}. \quad (6)$$

Within the minimal variants of the sterile neutrino model we are concentrated on, the signal fluxes are constrained from above by upper limits on mixing angle θ [entering Eq. (5)] placed by previous x-ray experiments. Likewise the fluxes are constrained from below by coming from cosmology lower limits on mixing angle. Hence, for each astrophysical source the expected from the dark matter decays flux is bounded from above and from below.

With limits depicted in Fig. 1, we estimate the x-ray signal flux (5) for each source, assuming background model in Sec. III. For the *eROSITA* observation of GC with radius of 60° we cut the central part of 2.5° radius and

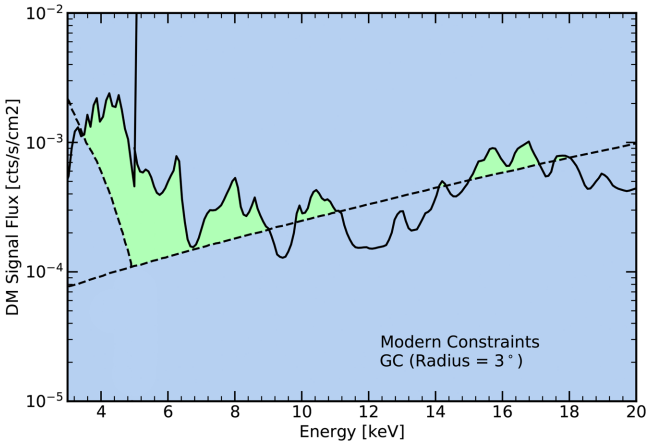

FIG. 5. The allowed region of the possible signal flux (5) (green) from decays of dark matter particles, which can be tested with the *eROSITA* and *ART-XC* telescopes on board *SRG* observatory in GC pointed observations (the circular region of radius 3°). The regions in blue are already excluded from x-ray telescopes (regions above the solid lines) and cosmology assuming the resonant mechanism responsible for the sterile neutrino production in the early Universe (regions below the dashed lines).

the Galactic disc of ±1.5°. Figure 5 illustrates the possible signal flux from observations of the GC: any peaklike feature in the x ray with parameters (flux and energy) inside the green region may hint at its dark matter nature within the described sterile neutrino model. We use the estimated fluxes to evaluate the observation time T, required to strengthen the existing limits (i.e., to enter the green regions similar to that in Fig. 5). Namely, observation for a period T allows one to place a limit on photon flux $F_{\rm DM}$ at a confidence level (in terms of the standard deviation σ) if the expected flux is not detected:

$$T = \left[\frac{F_{\rm DM} \times G(E)/\Omega + C_{\rm BG}}{F_{\rm DM}^2 \times G^2(E)/\Omega^2}\right]\sigma^2, \tag{7}$$

where $G(E)/\Omega$ is the ratio of grasp to angular size of the source, and $C_{\rm BG}$ is the background count rate (in counts per second). Note that this equation is valid only in case when source angular size is larger than the telescope FOV. If one observes a region equal to the field of view of the telescope ($\Omega \cong$ FOV), then this ratio is the effective area (EA) of the telescope. With *SRG* survey strategy (see Sec. III), both *ART-XC* and *eROSITA* sky coverage inside the cones centered on GC can be considered for our purpose as approximately uniform even for 60° cone radius. The count rate of the background events $C_{\rm BG}$ here is taken in a bandwidth corresponding to the telescope energy resolution. The energy resolution of the *eROSITA* telescope remains almost constant, 2.3%, over the entire observation energy range [8]. The energy dependence of *ART-XC* telescope energy resolution is taken from [3].

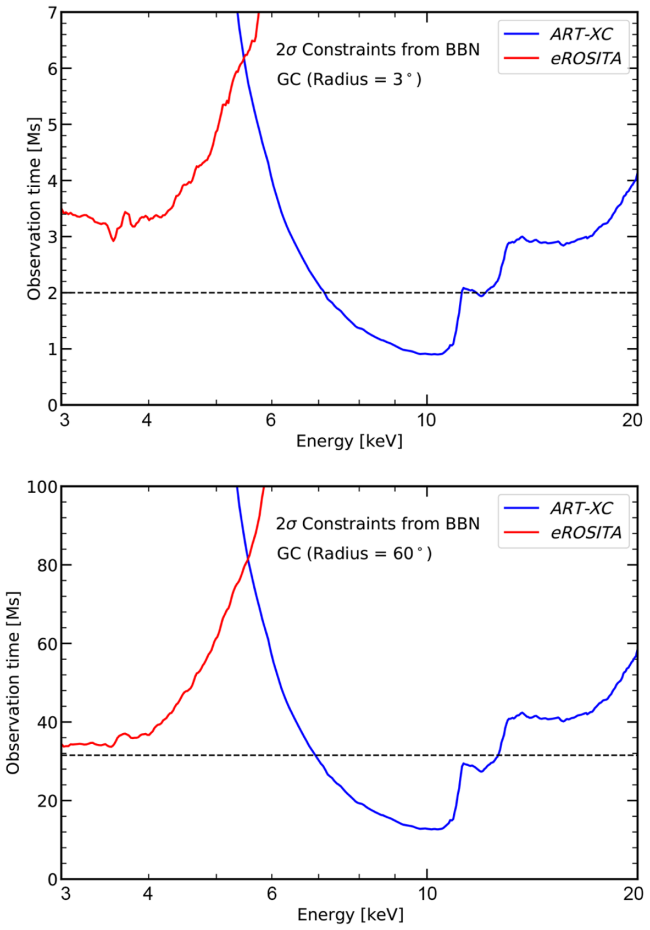

FIG. 6. The observation time for *eROSITA* and *ART-XC* telescopes for circular regions of radius 3° and 60° around the position of GC required to fully explore the dark matter sterile neutrino model with resonant production mechanism (exclusion at 2σ confidence level). The horizontal dashed line on the upper panel shows the exposure obtained by *ART-XC* observation of GC before the start of main survey program, the similar line on lower panel shows the exposure to be collected in the four-year *SRG* all-sky survey by each of the telescopes, *eROSITA* and *ART-XC*.

Figure 6 shows the estimated exposure time for the GC (in circular regions of radius 3° and 60°) with the *eROSITA* and *ART-XC* telescopes. It follows from (7) for placing a 2σ limit on the model with the lowest possible mixing sill yielding the dark matter sterile neutrinos via the resonant production in the early Universe and consisting with cosmological constraints from the BBN. Horizontal dashed lines in Fig. 6 show the exposure time achievable with *SRG* telescopes in various sky surveys (see discussion below).

V. CONCLUSIONS AND OUTLOOK

In this paper, we examined the capabilities of the *SRG* mission to detect a signal from the dark matter formed by sterile neutrinos, which can decay into active neutrino and

photon. We have estimated the potential signal fluxes which can be detected during the *SRG* mission from the Galactic Center, and the Andromeda and Draco galaxies. For the Milky Way, we separately examined the expected signal flux for two different observational strategies: the observations near the Galactic Center (3° radius towards the center) and in the periphery of the Milky Way (60° radius around the GC). Based on these data, we estimated the necessary exposure time to observe the Milky Way in these two cases for a reliable exclusion of the lowest possible signal from decays of the dark matter sterile neutrinos resonantly produced in the early Universe. The modeling of the background spectra presented in this article does not contain possible systematic uncertainties. The results we offer provide only an assessment of the usefulness of *SRG* data in sterile neutrino decay studies. One more source of uncertainties is associated with variance of the DM profiles of the chosen halos, which can change the signal flux roughly by a factor of two. The numerical estimates presented below do not account for this uncertainty.

Remarkably, the estimated exposure time in case of the observations near the GC is comparable with the exposure of *ART-XC* GC survey, which was carried out in September 2019, shortly after the launch of the *SRG* spacecraft, during the performance and verification observations phase. In this survey ≈40 square degrees region around GC was covered by the *ART-XC* for nearly 24 days (≈2 Ms, shown as the horizontal dashed line on the upper panel of Fig. 6). Using these data it should be possible to obtain stronger than 2-σ constraints on the lowest possible dark matter decay signal at the photon energies between 5.5 and 19 keV. Unfortunately, only a few *eROSITA* detectors were occasionally switched on in the testing mode during these observations, so the possibility to obtain strong dark matter decay constraints using these *eROSITA* data should be still investigated.

The exposure time in a wide 60° radius region towards the GC is to be compared to the exposure that will be obtained in the *SRG* all-sky survey. It is currently planned that all the sky will be surveyed by *SRG* during four years in total. Therefore, 60° radius circular region centered on the GC will be surveyed for approximately one year during this survey (≈30 Ms, shown as the horizontal dashed line on the lower panel of Fig. 6). These data will allow one to place stronger than 2-σ bounds on the lowest possible dark matter decay signal at the photon energies between 6.5 and 12.5 keV with *ART-XC* and at the photon energies below 6 keV with *eROSITA*. Thus, our estimates imply that it will be possible to obtain even stronger constraints on the parameters of sterile neutrinos in the corresponding mass range using the *ART-XC* and *eROSITA* all-sky data.

To illustrate this conclusion, we present in Fig. 7 limits on the mixing angle to be placed by *SRG* (assuming no signal is observed) with already collected data towards GC (only *ART-XC*, solid blue line), and with one-year [blue (red) dashed line for *eROSITA* (*ART-XC*)] and four-year survey data [blue (red) dotted blue line for *eROSITA* (*ART-XC*)] considering 60° region around GC. In particular, to detect at a 5-σ level the 7 keV dark matter sterile neutrino with mixing of about $\sin^2 2\theta \sim 5 \times 10^{-11}$ (invited to explain the anomalous 3.5 keV line [27,28]), it takes only ∼25 ks and 0.4 Ms of observations near GC and in the wide angle around GC, respectively. The *eROSITA* sensitivity at 3.5 keV is approximately similar to that of *XMM*-Newton, as expected, see, e.g., [31], also Fig. 4. Confronting these exposures with *SRG* mission time scale one concludes, that the constraints to be obtained by the *eROSITA* telescope near the 3.5 keV line signal reported earlier can be comparable to that obtained from *XMM*-Newton data, which will provide with another independent study of the possible sterile neutrino decay signal in this mass range. Similar and higher sensitivities to the sterile neutrino model are expected for the next generation x-ray telescopes like *Athena* and *eXTP*, see, e.g., [57,58].

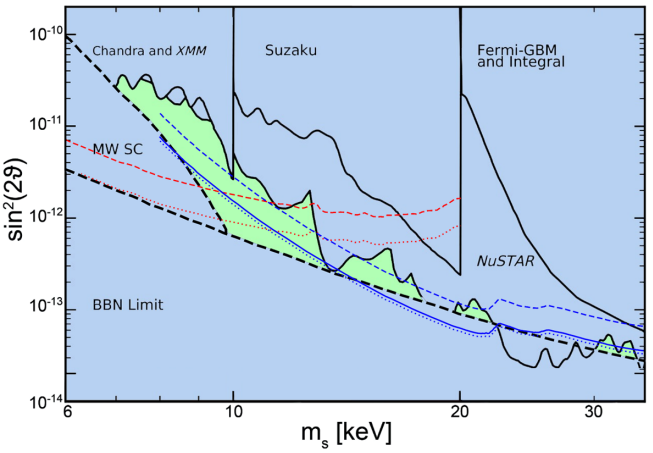

FIG. 7. The expected limits on the sterile neutrino model parameter space to be obtained (assuming no signal) with already collected data towards the GC (solid line) and with data to be collected after one year (dashed line) and four years (dotted line) of operation in the all-sky survey mode and used to analyze the signal from 60° region around the GC. Red (blue) lines refer to *eROSITA* (*ART-XC*) instruments; black solid and dashed lines indicate existing constraints, the same as in Fig. 1.

At the photon energies below approximately 2.4 keV the *eROSITA* sensitivity in wide angle observations is higher than that of *XMM*-Newton. Therefore *eROSITA* data from a wide circular region around GC yields a new independent prob of the region of the DM sterile neutrino parameter space, previously disfavored from the Milky Way satellite counts [59], not from x-ray observations. This may be important, since both methods may have their own unknown systematics. Likewise, if dark matter particles decay, it happens in each galaxy and all the time, so the expected x-ray signal from unresolved astrophysical sources at cosmological distances suffers from redshifting and correlates with the cosmic structure. The sensitivity of

the *eROSITA* to the corresponding observables in the x-ray diffuse all-sky map has been studied in Refs. [60,61]. Similar investigation is envisaged for *ART-XC*. As a kind of intermediate approach, one can use the stacked spectra of resolved astrophysical sources to search for the decay signature.

The data of x-ray surveys (full sky coverage) that are carried out with *ART-XC* and *eROSITA* telescopes aboard the *SRG* space observatory will give a possibility to fully explore the dark matter sterile neutrino model with resonant production in the early Universe. The presence of overlapping areas in the energy ranges of the *eROSITA* and *ART-XC* telescopes will further improve the overall sensitivity to the parameters of sterile neutrinos. The *SRG* mission has high potential for verifying the dark matter sterile neutrino hypothesis within the minimal extensions of the SM like νMSM [62], where no additional ingredients are introduced in the model to change the neutrino dynamics at the production epoch. There still be a room for the models with sterile neutrino forming only a fraction of dark matter. To conclude, the *SRG* mission has a very high potential for testing the sterile neutrino dark matter hypothesis.

ACKNOWLEDGEMENTS

Authors are grateful to Eugene Churazov, Oleg Ruchayskiy, and Mikhail Shaposhnikov for useful discussion and important comments. The work on theoretical prediction of DM signal from decaying sterile neutrinos is supported by the Russian Science Foundation (RSF) Grant No. 17-12-01547. Calculation of the sensitivity of x-ray telescopes in wide-angle observations is done under support of the RSF Grant No. 18-12-00520.

[1] R. Sunyaev *et al.*, Astron. Astrophys. (to be published).
[2] M. Pavlinsky, V. Akimov, V. Levin, I. Lapshov, A. Tkachenko, N. Semena, V. Arefiev, A. Glushenko, A. Yaskovich, R. Burenin *et al.*, SPIE Int. Soc. Opt. Eng. **8147**, 814706 (2011).
[3] M. Pavlinsky, A. Tkachenko, V. Levin, A. Krivchenko, A. Rotin, M. Kuznetsova, I. Lapshov, R. Krivonos, A. Semena, N. Semena *et al.*, Exp. Astron. **45**, 315 (2018).
[4] M. Pavlinsky, A. Tkachenko, V. Levin, A. Krivchenko, A. Rotin, M. Kuznetsova, I. Lapshov, R. Krivonos, A. Semena, N. Semena *et al.*, Exp. Astron. **47**, 1 (2018).
[5] M. Pavlinsky, A. Tkachenko, V. Levin, A. Krivchenko, A. Rotin, M. Kuznetsova, I. Lapshov, R. Krivonos, A. Semena, N. Semena *et al.*, Exp. Astron. **48**, 233 (2019).
[6] M. Pavlinsky *et al.*, Astron. Astrophys. (to be published).
[7] P. Predehl, R. Andritschke, H. Böhringer, W. Bornemann, H. Bräuninger, H. Brunner, M. Brusa, W. Burkert, V. Burwitz, N. Cappelluti *et al.*, SPIE Int. Soc. Opt. Eng. **7732**, 77320U (2010).
[8] A. Merloni, P. Predehl, W. Becker, H. Böhringer, T. Boller, H. Brunner, M. Brusa, K. Dennerl, M. Freyberg, P. Friedrich *et al.*, arXiv:1209.3114.
[9] P. Predehl, R. Andritschke, V. Arefiev, V. Babyshkin, O. Batanov, W. Becker, H. Böhringer, A. Bogomolov, T. Boller, K. Borm *et al.*, Astron. Astrophys. **647**, A1 (2020).
[10] M. Pavlinsky, R. Sunyaev, E. Churazov, A. Vikhlinin, S. Sazonov, M. Revnivtsev, V. Arefiev, I. Lapshov, V. Akimov, V. Levin *et al.*, SPIE Int. Soc. Opt. Eng. **7437**, 743708 (2009).
[11] A. Pillepich, T. H. Reiprich, C. Porciani, K. Borm, and A. Merloni, Mon. Not. R. Astron. Soc. **481**, 613 (2018).
[12] A. Vikhlinin, A. V. Kravtsov, R. A. Burenin, H. Ebeling, W. R. Forman, A. Hornstrup, C. Jones, S. S. Murray, D. Nagai, H. Quintana *et al.*, Astrophys. J. **692**, 1060 (2009).
[13] P. A. R. Ade, N. Aghanim, M. Arnaud, M. Ashdown, J. Aumont, C. Baccigalupi, A. J. Banday, R. B. Barreiro, J. G. Bartlett *et al.* (Planck Collaboration), Astron. Astrophys. **594**, A24 (2016).
[14] T. Abbott, M. Aguena, A. Alarcon, S. Allam, S. Allen, J. Annis, S. Avila, D. Bacon, A. Bermeo *et al.* (DES Collaboration), Phys. Rev. D **102**, 023509 (2020).
[15] P. B. Pal and L. Wolfenstein, Phys. Rev. D **25**, 766 (1982).
[16] V. D. Barger, R. J. N. Phillips, and S. Sarkar, Phys. Lett. B **352**, 365 (1995); **356**, 617(E) (1995).
[17] K. Abazajian, G. M. Fuller, and W. H. Tucker, Astrophys. J. **562**, 593 (2001).
[18] M. Drewes *et al.*, J. Cosmol. Astropart. Phys. 01 (2017) 025.
[19] A. Boyarsky, M. Drewes, T. Lasserre, S. Mertens, and O. Ruchayskiy, Prog. Part. Nucl. Phys. **104**, 1 (2019).
[20] K. Abazajian *et al.*, arXiv:1204.5379.
[21] B. M. Roach, K. C. Y. Ng, K. Perez, J. F. Beacom, S. Horiuchi, R. Krivonos, and D. R. Wik, Phys. Rev. D **101**, 103011 (2020).
[22] S. Dodelson and L. M. Widrow, Phys. Rev. Lett. **72**, 17 (1994).
[23] X.-D. Shi and G. M. Fuller, Phys. Rev. Lett. **82**, 2832 (1999).
[24] M. Shaposhnikov and I. Tkachev, Phys. Lett. B **639**, 414 (2006).
[25] F. Bezrukov and D. Gorbunov, Phys. Lett. B **736**, 494 (2014).
[26] F. Bezrukov, A. Chudaykin, and D. Gorbunov, Phys. Rev. D **99**, 083507 (2019).
[27] E. Bulbul, M. Markevitch, A. Foster, R. K. Smith, M. Loewenstein, and S. W. Randall, Astrophys. J. **789**, 13 (2014).
[28] A. Boyarsky, O. Ruchayskiy, D. Iakubovskyi, and J. Franse, Phys. Rev. Lett. **113**, 251301 (2014).
[29] M. E. Anderson, E. Churazov, and J. N. Bregman, Mon. Not. R. Astron. Soc. **452**, 3905 (2015).

[30] F. A. Aharonian, H. Akamatsu, F. Akimoto, S. W. Allen, L. Angelini, K. A. Arnaud, M. Audard, H. Awaki, M. Axelsson, A. Bamba *et al.*, Astrophys. J. Lett. **837**, L15 (2017).
[31] C. Dessert, N. L. Rodd, and B. R. Safdi, Science **367**, 1465 (2020).
[32] J. F. Navarro, C. S. Frenk, and S. D. M. White, Astrophys. J. **462**, 563 (1996).
[33] K. Perez, K. C. Y. Ng, J. F. Beacom, C. Hersh, S. Horiuchi, and R. Krivonos, Phys. Rev. D **95**, 123002 (2017).
[34] W. Dehnen, D. McLaughlin, and J. Sachania, Mon. Not. R. Astron. Soc. **369**, 1688 (2006).
[35] A. Tamm, E. Tempel, P. Tenjes, O. Tihhonova, and T. Tuvikene, Astron. Astrophys. **546**, A4 (2012).
[36] A. Geringer-Sameth, S. M. Koushiappas, and M. Walker, Astrophys. J. **801**, 74 (2015).
[37] C. Karwin, S. Murgia, S. Campbell, and I. Moskalenko, Proc. Sci., ICRC2019 (**2019**) 570 [arXiv:1903.10533].
[38] S. Riemer-Sorensen and S. H. Hansen, Astron. Astrophys. **500**, L37 (2009).
[39] A. B. Pace and L. E. Strigari, Mon. Not. R. Astron. Soc. **482**, 3480 (2019).
[40] M. C. Smith *et al.*, Mon. Not. R. Astron. Soc. **379**, 755 (2007).
[41] M. Cautun, A. Benitez-Llambay, A. J. Deason, C. S. Frenk, A. Fattahi, F. A. Gómez, R. J. J. Grand, K. A. Oman, J. F. Navarro, and C. M. Simpson, Mon. Not. R. Astron. Soc. **494**, 4291 (2020).
[42] K. N. Abazajian, S. Horiuchi, M. Kaplinghat, R. E. Keeley, and O. Macias, Phys. Rev. D **102**, 043012 (2020).
[43] J. Diemand, M. Kuhlen, P. Madau, M. Zemp, B. Moore, D. Potter, and J. Stadel, Nature (London) **454**, 735 (2008).
[44] K. C. Y. Ng, B. M. Roach, K. Perez, J. F. Beacom, S. Horiuchi, R. Krivonos, and D. R. Wik, Phys. Rev. D **99**, 083005 (2019).
[45] F. Jansen, D. Lumb, B. Altieri, J. Clavel, M. Ehle, C. Erd, C. Gabriel, M. Guainazzi, P. Gondoin, R. Much *et al.*, Astron. Astrophys. **365**, L1 (2001).
[46] F. A. Harrison, W. W. Craig, F. E. Christensen, C. J. Hailey, W. W. Zhang, S. E. Boggs, D. Stern, W. R. Cook, K. Forster, P. Giommi *et al.*, Astrophys. J. **770**, 103 (2013).
[47] A. Neronov, D. Malyshev, and D. Eckert, Phys. Rev. D **94**, 123504 (2016).
[48] A. Gonzalez-Riestra and P. Rodriguez-Pascual, Tech. Report No. 3.12, XMM-SOC User Support Group, ESA/ESAC Spain, https://xmmweb.esac.esa.int/docs/documents/GEN-TN-0014.pdf (2019).
[49] M. Revnivtsev, S. Sazonov, M. Gilfanov, E. Churazov, and R. Sunyaev, Astron. Astrophys. **452**, 169 (2006).
[50] R. Krivonos, M. Revnivtsev, E. Churazov, S. Sazonov, S. Grebenev, and R. Sunyaev, Astron. Astrophys. **463**, 957 (2007).
[51] M. Revnivtsev, S. Sazonov, E. Churazov, W. Forman, A. Vikhlinin, and R. Sunyaev, Nature (London) **458**, 1142 (2009).
[52] K. Perez, R. Krivonos, and D. R. Wik, Astrophys. J. **884**, 153 (2019).
[53] D. H. Lumb, R. S. Warwick, M. Page, and A. De Luca, Astron. Astrophys. **389**, 93 (2002).
[54] A. Moretti, S. Campana, D. Lazzati, and G. Tagliaferri, Astrophys. J. **588**, 696 (2003).
[55] R. Launhardt, R. Zylka, and P. G. Mezger, Astron. Astrophys. **384**, 112 (2002).
[56] F. M. Fornasini, J. A. Tomsick, A. Bodaghee, R. A. Krivonos, H. An, F. Rahoui, E. V. Gotthelf, F. E. Bauer, and D. Stern, Astrophys. J. **796**, 105 (2014).
[57] A. Neronov and D. Malyshev, Phys. Rev. D **93**, 063518 (2016).
[58] D. Malyshev, C. Thorpe-Morgan, A. Santangelo, J. Jochum, and S.-N. Zhang, Phys. Rev. D **101**, 123009 (2020).
[59] J. F. Cherry and S. Horiuchi, Phys. Rev. D **95**, 083015 (2017).
[60] F. Zandanel, C. Weniger, and S. Ando, J. Cosmol. Astropart. Phys. 09 (2015) 060.
[61] A. Caputo, M. Regis, and M. Taoso, J. Cosmol. Astropart. Phys. 03 (2020) 001.
[62] A. Boyarsky, O. Ruchayskiy, and M. Shaposhnikov, Annu. Rev. Nucl. Part. Sci. **59**, 191 (2009).